DETECTING DIFFUSE CO_2 EMISSIONS ALONG THE NGAPOURI FAULT USING A TUNABLE DIODE LASER

Agnes Mazot[1], Andrew Rae[1] and Anna Jentsch[1,2]

[1] GNS Science, Wairakei Research Centre, 114 Karetoto Road, Wairakei RD4, Taupo, New Zealand

[2] Institute of Earth and Environmental Science, University of Potsdam, 14476 Potsdam, Germany

a.mazot@gns.cri.nz

Keywords: *Tunable Diode Laser, geothermal CO_2 mixing ratio measurements, Ngapouri Fault, Waiotapu-Waikite geothermal system.*

ABSTRACT

CO_2 mixing ratio measurements have been performed for the first time on the margins of Waiotapu geothermal area using an open-path Tunable Diode Laser (TDL). The survey measurements were conducted along strands of the Ngapouri Fault that extend to the south-southwest away from Waiotapu. The main purpose of these surveys was to test whether geothermal CO_2 mixing ratios can be detected along Ngapouri Fault strands where geothermal surface activity (e.g., sinter deposits and/or areas of steaming ground) is not observed. High CO_2 mixing ratios were observed at the top of some fault strands (474 ± 5 ppmv) and suggested that the Waiotapu-Waikite geothermal system extends at depth, southwards along the Ngapouri fault to small areas of geothermal surface activity.

1. INTRODUCTION

The purpose of this paper is to test whether geothermal-derived CO_2 gas can be detected along splays of the Ngapouri Fault where no obvious geothermal surface activity is observed. The Ngapouri Fault controls the location of several phreatic explosion craters and hydrothermal surface features along its length, indicating that it is a major structural control of deep geothermal fluid upflow in the area (Hedenquist and Henley, 1985). Craters and geothermal features proximal to the fault in our survey area include a fumarolic area on the eastern flanks of Maungaongaonga, a large explosion crater occupied by Lake Ngapouri, and an area of steaming, altered ground at the fault's southwestern extent (the Ngapouri geothermal areas; Figure 1). CO_2 is an effective tracer of subsurface geothermal activity and previous studies have suggested that hydrothermal eruptions both at Waiotapu and along the trace of the Ngapouri Fault were triggered by CO_2 gas pulses derived from the intrusion of basalt dikes at depth during the AD1315 Kaharoa magmatic eruptions (Nairn et al., 2005).

This paper introduces the preliminary results of CO_2 mixing ratio measurements made close to active geothermal areas along several strands of the Ngapouri Fault, where no geothermal surface features are obvious. CO_2 "mixing ratios" are measured in units of ppmv and remain constant with air density changes. Measurements were made between May and July 2014 as four transects across the fault traces. The transects are located southwest of the Maungaongaonga fumarolic areas, between Lake Ngapouri and the Ngapouri geothermal areas. In the process of performing the measurements background atmospheric CO_2 mixing ratios were systematically carried out prior to commencing the fault transects.

2. GEOLOGICAL SETTINGS AND STUDY AREA

The Waiotapu Geothermal System is one of more than twenty geothermal systems in the Taupo Volcanic Zone (TVZ) on the North Island of New Zealand (Figure 1; Bibby et al., 1995). With a surface area of around 17 km^2 and an average heat discharge of about 545 MW (DSIR Bulletin 155, 1963) it is considered the largest geothermal field in New Zealand (Giggenbach et al., 1994; NZGA) with a high diversity of surface geothermal features, such as geysers, large thermal springs (Champagne Pool), mud volcanoes and pools.

The Waikato Regional Council has classified the Waiotapu Geothermal Field as a protected system. In the past half century the area has been assessed by detailed geological surface mapping (DSIR Bulletin 155, 1963), and surveyed by geophysical techniques such as electrical resistivity (Figure 1: Stagpoole and Bibby, 1998; Risk et. al, 1994) and gravity measurements (DSIR Bulletin 155, 1963). Additionally, considerable work has been done on the stratigraphy of the Waiotapu system, and the origin of the various hydrothermal eruptions (Hedenquist and Henley, 1985), as well as the evolution of the geothermal system (Hedenquist and Browne, 1989). The southwest margin of the geothermal field is defined by Trig 8566, a rhyolite dome (Healy, 1974), and the lowlands of Reporoa Basin to the south (Grindley, 1963). To the northeast is Maungakakaramea and to the northwest, Maungaongaonga. Both are dacite volcanoes that are crossed by the northeast-striking Ngapouri Fault (Healy, 1974: Hedenquist and Henley, 1985).

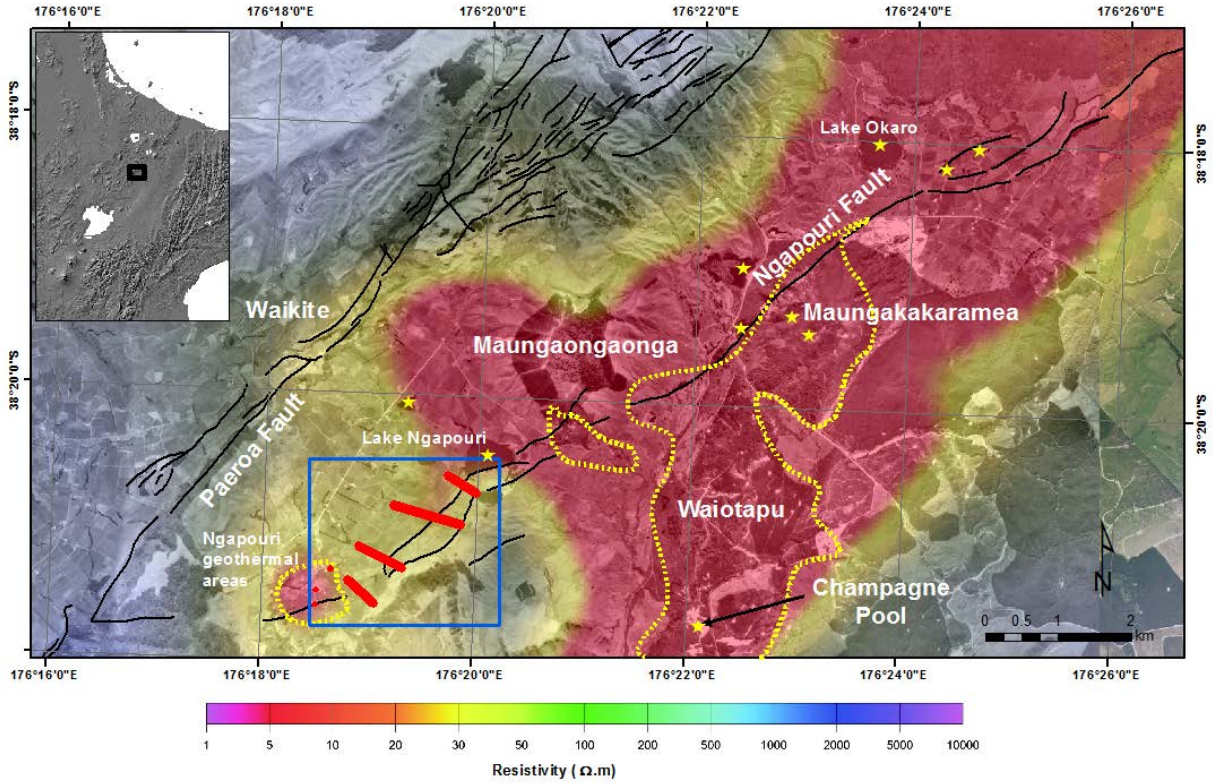

Figure 1: Aerial photograph showing mapped active faults (GNS Science active fault database), including the Ngapouri Fault, overlaid onto the electrical resistivity map (nominal array spacing 500 m) of Stagpoole and Bibby (1998). The yellow dashed lines enclose areas of active thermal ground. Yellow stars indicate some of the hydrothermal eruption centres defined by Hedenquist and Henley (1985). The blue rectangle indicates our survey area (shown in Figure 3), with the red lines being the locations of the CO_2 measurement traverses of the Ngapouri Fault strands.

As a major branch of the Paeroa Fault, the overall strike of the Ngapouri Fault (55°) follows the general trend of the Taupo Fault Belt (40°-60°) (Rowland and Sibson, 2001; Villamor and Berryman, 2001). With a length of about 15 km, this normal fault dips northwest, and passes from Paeroa Trig northeast across the hummocky slopes of Paeroa Range (Newson et al., 2002), along the eastern shore of Lake Ngapouri towards Lake Okaro (Grindley, 1963). The fault is known to displace >0.23 Ma ignimbrites (Nairn, 2002). Several hydrothermal explosion craters occur along its length (Figure 1; Healy, 1974; Hedenquist & Henley, 1985; Villamor & Berryman, 2001; Nairn et al., 2005). Although the fault scarps are poorly preserved, due to being partially buried by recent ash, in our study area, the scarp is defined by the southeastern uplifted block, which forms the gentle, northwest-facing slopes of the northeast-striking Ngapouri Ridge.

Previous studies (Villamor & Berryman, 2001; Nairn et al., 2005; Berryman et al., in prep) using excavated trenches across the Ngapouri Fault traces have mapped tephra layers and fault splays in the trench walls to measure fault displacements and estimate displacement rates (0.23 ± 0.001 mm/yr; Villamor and Berryman, 2001). These trenches provide excellent validation of fault locations in parts of our study area.

3. METHODOLOGY

3.1 The GasFinder tunable diode laser

The tunable diode laser spectroscopy (TDLS) technique consists of the measurement of gas mixing ratio based on the absorption of Infra-Red radiation by the target gas. TDLS is used for accurate measurement of a specific gas as it uses a light source this is tunable over a narrow wavelength range.

The TDL used in this study consists of a GasFinder 2.0 Tunable Diode Laser (Boreal Laser Inc), an Infra-Red transmitter/receiver (transceiver) unit that can be used to measure CO_2 mixing ratios over linear paths of up to 1 km distance. The laser source located in the transceiver is a near-infrared room temperature tunable diode laser operating at 1576.9 nm for CO_2 absorption line. A laser light emitted from the transceiver propagates through the atmosphere to a retro-reflector array (9 gold plated triple faced cubes) and returns to the transceiver where it is focused onto a photodiode detector. A part of the laser beam is passed through a reference cell (with known and stable CO_2 reference mixing ratio) located in the unit to have a continuous calibration update. These two signals are converted into electrical waveforms and then processed by an on-board computer to obtain CO_2 column amount (in ppm m) along the optical path. Linear concentrations are

converted into average CO_2 mixing ratios (in ppmv) along the path by the known path length. The accuracy of the measurement is evaluated by correlation coefficient (R^2), which is the measure of the similarity between the waveform of the signal passing through reference and the measured sample. According to the manufacture's datasheet, an accuracy of ± 2 % is achieved for R^2 >0.95 (Trottier et al, 2009).

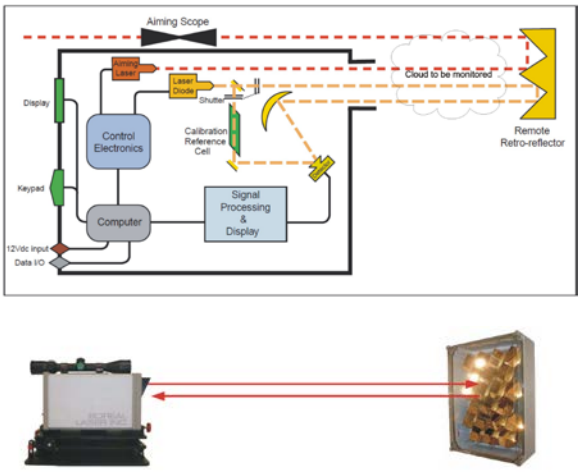

Figure 2: Schema of the Diode laser system with the transceiver and the retroreflector array (lower picture).

3.2 Experimental set-up

In the field, the GasFinder was set to measure CO_2 mixing ratios at a rate of 1 Hz. Alignment between the transceiver and the retro-reflector was optimized using a red visible aiming laser and a sighting scope. The size of the retroreflector array was based on optimisation of the level of returning light to a desired value, depending on the path-length and the expected amount of absorbed radiation. The light level is the amount of energy returned by the retroreflector and captured by the optics inside the GasFinder. This parameter is adimensional and can range between 500 and 16,000. During field operations, the desired working range (where the GasFinder behaves linearly) is between 4,000 and 8,000: at lower level (<2,000) there is a sensible loss of accuracy of the signal, while non-linear behavior can be attained for values > 12,000.

Figure 3 shows the locations of the four traverses across the Ngapouri Fault. The Ngapouri Fault strands were mapped using aerial photographs, locations confirmed in two locations from excavated trenches (Nairn et al., 2005; Berryman et al, in prep). The CO_2 measurements were made as traverses perpendicular to the mapped fault traces, starting a few hundred meters east of the fault and recording the CO_2 mixing ratios at 50 m path lengths. Traverses 2 and 3 are at the same location of trenches that were mapped by Berryman et al. (in prep) (long since filled-in; Figure 3), thus providing excellent definition of the location of the fault traces at these traverses.

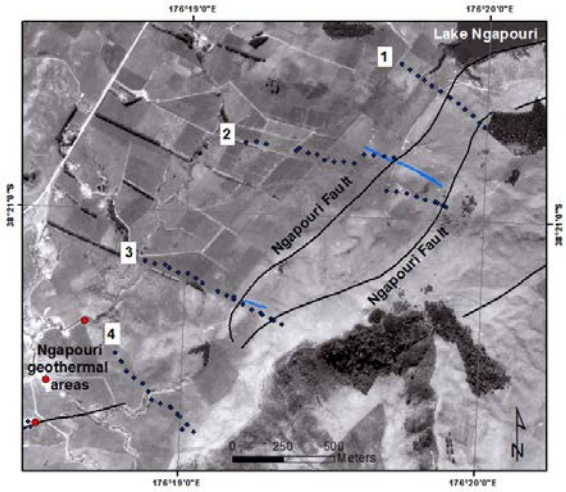

Figure 3: Location of the fault traverses, numbered 1 – 4. Blue diamonds are the Transceiver and the retroreflector positions. The red dots are areas of geothermal activity. The blue lines represent the location of the mapped trenches by Berryman et al. (in prep).

4. RESULTS

1.1 Background atmospheric CO_2 mixing ratio measurements

CO_2 mixing ratio measurements were made at Kinloch north of Lake Taupo (38°37′38″ S, 175°56′56″ E) in a paddock to establish a baseline for CO_2 mixing ratios well outside an active geothermal area. The mean atmospheric CO_2 mixing ratio was 394 ± 4 ppmv.

Other background measurements were made in the survey area, a few hundred metres from the Ngapouri Fault traces, but also away from any geothermal activity. The mean CO_2 mixing ratio was 404 ± 5 ppmv. These measurements were repeated at the same site a day later and found to have a mixing ratio of 410 ± 4 ppmv. These results are considered to be within error and demonstrate the repeatability of this method.

1.2 Influences on measurements

Atmospheric conditions (e.g. fog, wind, clouds) can influence the CO_2 mixing ratio measurements, as well as vegetation cover, geomorphology, operating vehicles and animal respiration (i.e., cows). Land use within the survey area is for grazing cattle, and this was something to be aware of if cattle were close by when measuring for atmospheric CO_2. When making CO_2 mixing ratio measurements, any of these influences (and possibly others) need to be taken into account.

1.3 Geothermal CO_2 mixing ratio measurements

Initial traverses were made at the Ngapouri geothermal area (Figure 3) across steaming ground and gas vents. The mean CO_2 mixing ratio at this location was 469 ppmv, with a minimum of 444 ppmv and a maximum of 554 ppmv.

Three traverses perpendicular to the fault were performed in the area between the Lake Ngapouri and the Ngapouri geothermal areas (Figure 3). No geothermal surface features are obvious at the traverse locations, although a small area

of gas venting is located 200 m northwest of Traverse 4 (Figure 3).

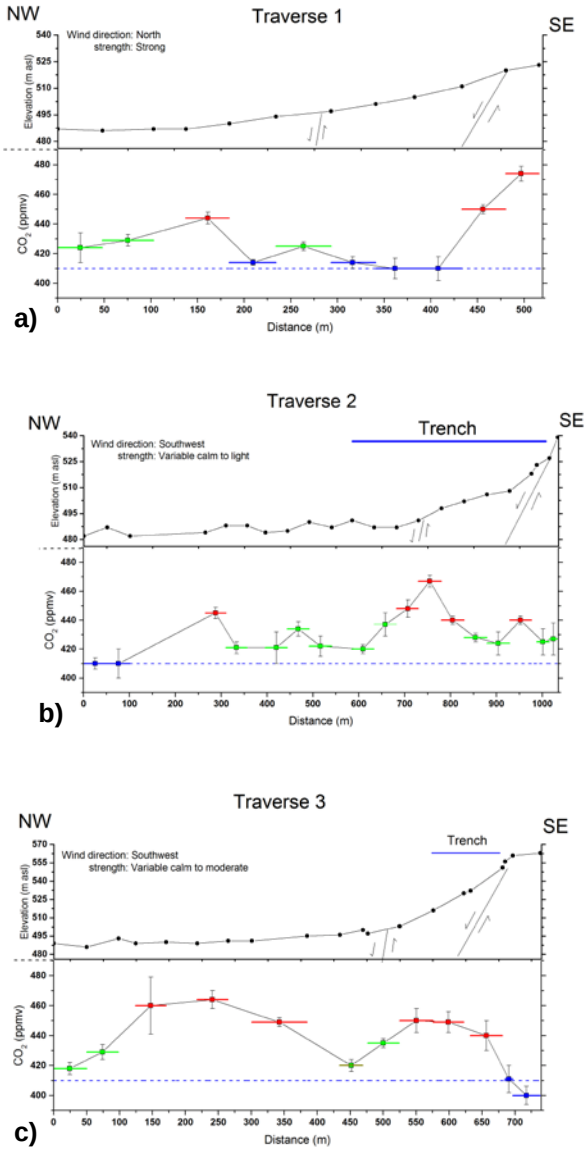

Figure 4: Traverses 1, 2 and 3 across the Ngapouri Fault (Figure 3), showing elevation (m asl), fault locations, locations of mapped trenches (for traverses 2 and 3) and measured CO_2 mixing ratios (ppmv) along each traverse. Each measurement is a CO_2 mixing ratio within the 50 m path length (represented as a coloured horizontal line), with a central point showing standard deviation mixing ratio errors bars. Mixing ratios for each measurement are colour coded: red = >440 ppmv, green = 420 – 440 ppmv, blue = < 420 ppmv. Dashed blue lines represent the mean background CO_2 mixing ratio (410 ppmv).

Measurements along Traverse 1, the most northerly traverse (Figure 3) and distal from areas of obvious geothermal activity, show good correlation with mapped fault traces. On the day of measurements, wind direction was from the north. The highest CO_2 mixing ratios, with a maximum of 450 and 474 ppmv, occur directly above the eastern splay, but they are also above background mixing ratios (425 ± 3 ppmv) across the mapped western splay (Figure 4a). However, elevated mixing ratios (444 ± 4 ppmv) are also found west of the mapped fault traces.

Approximately 500 m southwest of Traverse 1, Traverse 2 is at the same location as the excavated trench (Fig. 3; Berryman et al., in prep.). On the day of measurements the wind direction was from the southwest. This traverse shows elevated CO_2 mixing ratios across the mapped fault traces, with highest mixing ratios (467 ± 4 ppmv) over the western splay and mixing ratios above background across the eastern splay (440 ± 3 ppmv; Fig. 4b). However, as with Traverse 1, elevated gas mixing ratios (445 ± 4 ppmv) are also measured west of the mapped faults.

Traverse 3 is located approximately 800 m southwest of Traverse 2, ~450 m northeast of the closest active geothermal area (Figure 3). On the day of measurements, wind direction was from the southwest. Elevated CO_2 mixing ratios occur above, and between, the mapped fault traces. However the highest mixing ratios (464 ± 6 ppmv) along this transect occur west of the mapped faults (Figure 4c).

Traverse 4 is located approximately 550 m southwest of Traverse 3, and is the closest to the Ngapouri geothermal areas (the northwestern end of the traverse is ~300 m from an area of steaming ground; Figure 3). This traverse is across an area where there are no mapped fault traces. However, projection of the mapped traces across this area would place the fault close to a ~5 m step in the elevation profile (Figure 5). On the day of measurements, the wind direction was from the southwest. Highest mixing ratios (440 ± 8 ppmv) along this traverse occur above the projected location of the fault trace (Figure 5). However, elevated mixing ratios (436 ± 7 ppmv) are also present at 4 measurement locations towards the west.

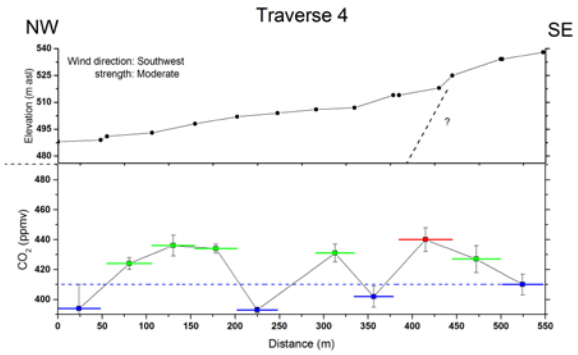

Figure 5: Traverse 4 across an area between mapped splays of the Ngapouri Fault (Figure 3), showing elevation (m asl), possible fault location and measured CO_2 mixing ratios (ppmv) along the traverse. Each measurement is a CO_2 mixing ratio within the 50 m path length (represented as a coloured horizontal line), with a central point showing standard deviation mixing ratio errors bars. Mixing ratios for each measurement are colour coded: red = >440 ppmv, green = 420 – 440 ppmv, blue = < 420 ppmv. Dashed blue lines represent the mean background CO_2 mixing ratio (410 ppmv).

5. DISCUSSION AND CONCLUSIONS

The Ngapouri Fault is regarded to have been a focus for the arrested intrusion of basalt dikes that triggered the AD1315 Kaharoa rhyolite eruptions from Tarawera volcanic vents, resulting in phreatic eruptions proximal to the length of the Ngapouri Fault (Nairn et al., 2002). This implies that this fault is a deeply penetrating structural feature that provides favourable permeability for the passage of upwelling geothermal fluids from depth to surface (Lloyd, 1959; Hedenquist and Browne, 1989).

The results of this study shows excellent correlation between elevated atmospheric CO_2 gas mixing ratios and the known, and projected, locations of Ngapouri Fault traces. This suggests that the fault is diffusely venting CO_2 gas along traces between surface geothermal areas located on Maungaongaonga, to the north, and the Ngapouri geothermal area to the southwest.

The Direct Current electrical resistivity map (AB/2 = 500 m) of the district shows a region of conductive rock extending from Waiotapu to Waikite in the west (Stagpoole and Bibby, 1998). The Waiotapu geothermal area is regarded to be hydrologically connected to the Waikite geothermal area, with the latter being a western outflow from the Waiotapu system (Bibby et al. 1994; Stewart, 1994). This hypothesis has recently been successfully modeled by Kaya et al. (2014). The implication is that a high temperature geothermal reservoir occurs at depth (i.e., at least ~250 m) east to west beneath the uplifted Paeroa Fault block. The results of our CO_2 mixing ratio measurements suggest that the Waiotapu – Waikite geothermal reservoir also extends towards the south, focused along the Ngapouri Fault, and include the small Ngapouri geothermal areas.

All four of the CO_2 traverses presented here consistently show elevated CO_2 mixing ratios at locations west of known mapped fault traces. It is possible that CO_2 is diffusely venting at unmapped fault splays. However, other sources should be considered. It is possible that CO_2 from areas of steam venting (i.e., the Ngapouri geothermal areas) has drifted across the measured path lengths. This is especially so for the Traverses 3 and 4, when the wind direction was from the southwest. Another possible source is from grazing cattle.

The benefits of using a TDLS for conducting atmospheric CO_2 mixing ratio measurements sourced from geothermal areas include:

- the sensitivity of the technique is able to measure small mixing ratios (i.e., 5 – 10 ppmv above background mixing ratios), and as such is useful for measuring diffusely venting CO_2;
- the equipment is portable and measurements are rapid;
- ability to cover wide areas, and then easily locate the source(s) of gas by systematically narrowing the path length;
- the measurements are made remotely, reducing the health and safety risk of working close to, and within active geothermal areas.

ACKNOWLEDGEMENTS

Pilar Villamor for valuable structural discussions and insights regarding the nature of the Ngapouri fault system. Kate McCallum and Karen Britten for assistance in the field with the CO_2 measurements. This project was funded through the NZ Geothermal Research Programme.

REFERENCES

Bibby, H.M., Caldwell, T.G., Davey, F.J., Webb, T.H.: Geophysical evidence on the structure of the Taupo Volcanic Zone and its hydrothermal circulation. *J. Volcanol. Geotherm. Res.*, 68, pp. 29-58. (1995).

Bibby, H.M., Bennie, S.L., Stagpoole, V.M., Caldwell, T.G.: Resistivity structure of the Waimangu, Waiotapu, Waikite and Reporoa geothermal areas, New Zealand. *Geothermics.*, 23, pp. 445-471. (1994).

Chianese, D.S., Rotz, C.A., Richard, T. L.: Simulation of carbon dioxide emissions from dairy farms to assess greenhouse gas reduction strategies. *Trans. ASABE*. 52, pp. 1301–1312. (2009).

DSIR Bulletin 155: Waiotapu Geothermal Field. D.S.I.R., New Zealand. pp. 141 (1963).

Giggenbach, W., Sheppard, D.S., Robinson, B.W., Stewart, M.K., Lyon, G.L.: Geochemical structure and position of the Waiotapu geothermal field, New Zealand. *Geothermics* 23 (5–6), pp. 599–644. (1994).

Grindley, G.: Geology and structure of Waiotapu geothermal field. Waiotapu geothermal field. *DSIR Bull.* 155, pp. 10–25. (1963).

Healy, J.: Waiotapu Geothermal Field. *NZ Geological Survey Report 38, Part D, Section 3(16)*, 6. (1974).

Hedenquist, J.W., Henley, R.W.: The evolution of the Waiotapu geothermal system, New Zealand, based on the chemical and isotopic composition of its fluids, minerals and rocks. *Geochim. Cosmochim. Acta.* 53, pp. 1640–1668. (1985).

Hedenquist, J.W., Browne, P.R.L.: Hydrothermal eruptions in the Waiotapu geothermal system, New Zealand: their origin, associated breccias and relation to precious metal mineralization. *Econ Geol* 80, pp. 2235–2257. (1989).

Kaya, E., O'Sullivan, M.J., Hochstein, M.P.: A three-dimensional numerical model of the Waiotapu, Waikite and Reporoa geothermal areas, New Zealand. *J. Volc. Geotherm. Res.* 283, 127-142 (2014)

Lloyd, E.F.: The hot springs and hydrothermal eruptions of Waiotapu. *N.Z. J. Geol. Geophys.*, 2, pp. 141-176. (1959).

Nairn, I.A.: Geology of the Okataina Volcanic Centre, 1:50 000. Institute of Geological and Nuclear Sciences geological map 25. 1 sheet + 156 p. IGNS Ltd., Lower Hutt, New Zealand. (2002).

Nairn, I.A., Hedenquist, J.W., Villamor, P., Berryman, K.R., Shane, P.A.: The ~AD1315 Tarawera and Waiotapu eruptions, New Zealand: contemporaneous rhyolite and hydrothermal eruptions driven by an

arrested basalt dike system? *Bull Volcanol* 67, 186-193 (2005), DOI 10.1007/s00445-004-0373-7.

Newsom, A., Prebble, W.M., Browne, P.R.L.: Landsliding on the Paeroa Fault at Te Kopia. *Proc. of the 24th New Zealand Geothermal Workshop*, pp. 119-124. (2002).

Rowland, J.V., Sibson, R.H.: Extensional fault kinematics within the Taupo Volcanic Zone, New Zealand: soft-linked segmentation of a continental rift system. *N.Z. J. Geol. Geophys.*, 44, pp. 271–283. (2001).

Risk, G.F., Caldwell, T.G., Bibby, H.M.: Deep resistivity surveys in the Waiotapu–Waikite–Reporoa region, New Zealand. *Geothermics* 23 (5–6), pp. 423–443. (1994).

Stagpoole, V.M., Bibby, H.M.: Electrical resistivity map of the Taupo Volcanic Zone, New Zealand; nominal array spacing 500 m, 1:250 000, version 1.0. Institute of Geological and Nuclear Sciences geophysical map 11. IGNS Ltd., Lower Hutt, New Zealand. (1998).

Stewart, M.K.: Groundwater contributions to Waikite geothermal fluids. Proc. 16th New Zealand Geothermal Workshop, Auckland, New Zealand. pp. 109-114. (1994).

Trottier S, Gunter, W.D., Kadatz, B., Olson, M., Perkins, E.H.: Atmospheric monitoring for the Pembina Cardium CO_2 monitoring project using open path laser technology. *Energy Procedia*, 1, pp. 2307–2314. (2009).

Villamor, P., Berryman, K.: A late Quaternary extension rate in the Taupo Volcanic Zone, New Zealand, derived from fault slip data. *N.Z. J. Geol. Geophys.*, 44, pp. 243-270. (2001).